Mesoscopic characterization of allotropic transformation in iron

N. BRUZY [a], M. CORET [a], L. STAINIER [a], B. HUNEAU [a]

a. Institut de Recherche en Génie Civil et Mécanique (GeM)
Ecole Centrale de Nantes, Université de Nantes, CNRS UMR 6183
1 rue de la Noë BP 92101 44321 Nantes cedex 3, France

Abstract :

This work focuses on in situ observation of ferrite-austenite allotropic transformation in iron. An in-house device is designed to capture images of a sample at mesoscale during phase change. Mechanical fields on the surface of the sample may then be computed thanks to the Digital Image Correlation technique. Experimental strain field can be compared directly to results from finite element simulations obtained from a coupled model formulated in a variational framework.

Keywords : Digital Image Correlation, Allotropic Transformation, Variational Framework

1 Introduction

Ferrite to austenite transformation in iron involves a change from a BCC to a FCC crystal structure and a lattice parameter reduction from 0.365 nm to 0.291 nm [1]. The associated change of compacity is thus responsible for local mechanical deformations around transformation sites. Traditional transformation characterization methods fail to highlight this feature. Indeed, macroscopic methods such as dilatometry lead to an averaging of transformation phenomena over the whole sample whereas in-situ observation methods - for instance laser scanning confocal microscopy technique - do not allow extracting information on the evolution of mechanical fields during the transformation.
The main objective of this work is to come up with a new experimental testing method that would permit to both monitor microstructural changes during the allotropic transformation and measure their effects on mechanical fields. Contacting methods for deformation measurement, such as strain gauges and extensometers, have been discarded as they only allow doing local measurements and may damage the samples at high temperatures. Among non-contacting techniques, Digital Image Correlation (DIC) has been selected due to its rather simple experimental set-up and the high resolution that can be attained. Besides, DIC has been proven reliable at high temperatures for a wide variety of materials and applications [2, 3, 4]. However, in order to highlight the different steps of the allotropic transformation it is necessary to acquire subgrain-resolution in situ images of the surface of a sample. Such kind of observation remains challenging owing to the necessity to combine high resolution imaging and adaptability to high temperatures.

2 Design of an experimental set-up for the characterization of allotropic transformation

2.1 Heating system

Choice has been made to design a home-made experimental device to maximize image resolution and keep control over thermal solicitation imposed to the sample. Classical heating methods are induction heating, Joule heating and furnace heating. Joule heating is preferred on account for the easy access to the sample it provides, the possibility to impose fast variations of temperature and its volumetric character. This latter aspect implies in particular that there is no temperature gradient inside the studied zone of the sample. A 5kW power supply with 500A maximum current provides the electrical current. The maximum heating rate that can be achieved is around 500°C/s. Temperature of the sample is measured by means of a 2-color pyrometer. A PID regulation is synthesized for the temperature to follow imposed profiles.

2.2 Sample protection

Following pioneering works on DIC at high temperatures [5, 6], several precautions are taken to avoid loss in image quality during testing since any modifications in the image properties could derail image correlation computations. In particular, degradation of sample surface may occur through oxidation. To avoid it, samples are put under an argon atmosphere. The experimental device is preliminarily pumped several times down to a 3 mbar vacuum using a rotary vane pump to clear the atmosphere from any residual that could be detrimental to the experiment.
The risk of keeping the sample under a gaseous atmosphere is that heat haze effect may occur : as the sample is heated, the temperature of the surrounding atmosphere is also raised, which locally modifies its refraction index. This induces small offsets that distort the images of the sample surface and that are very often assimilated to actual deformations by the correlation routine. To limit the influence of heat haze effect, a constant controlled flow of gas is maintained during the experimental tests. However no image distortion has been noticed so far.

2.3 Optical system

The surface of the sample radiates a light whose energy evolves with temperature. More precisely, blackbody radiative emission from the sample is ruled by Planck's law :

$$I(\lambda, T) = \frac{2hc^2}{\lambda^5} \frac{1}{exp^{\frac{hc}{\lambda kT}} - 1} \tag{1}$$

From this equation it may be seen that the intensity of emitted light rises quickly during heating, especially for high wavelengths. When thermal radiation gets brighter than the source of light used in the experiments, images luminosity exhibit strong variations that interfere with correlation results.
To tackle this problem, sample is lit by a blue LEDs illumination system that maintains lighting in the low wavelengths range. A blue filter is put in front of the camera to cut all wavelengths that are outside this work range. However, high intensities in the blue wavelengths due to thermal radiation are still to be expected at temperatures above 1000°C [6] but this level of temperatures is not considered in the scope of this work.

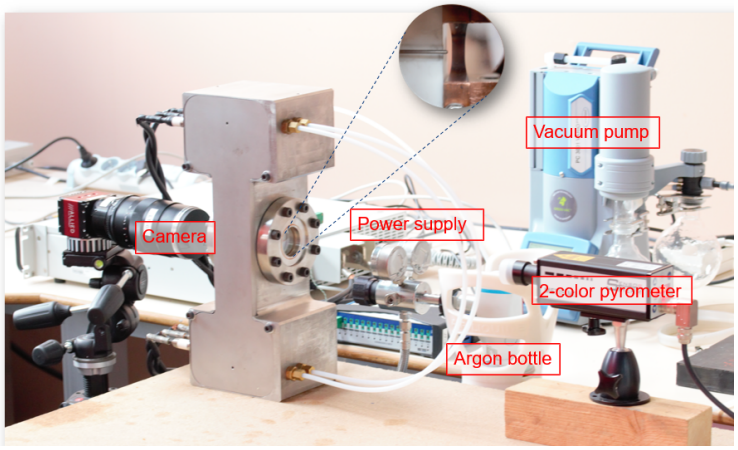

FIGURE 1 – Photography of the experimental set-up and detail view of the sample

2.4 General view of the set-up

Experimental set-up is shown in Figure 1 with a detail view on the sample. Experimental device consists of a box with electrical and fluid feedthroughs. The sample is maintained using two copper clamps. However, no effort should be exerted on the sample in reaction to its dilatation to prevent buckling. Consequently an operating clearance is preserved in the sample fixation so that the sample can freely dilate. There are two observation sapphire windows (0-deg orientation, 0.2λ flat, 50/20 surface polish). Temperature is measured on one side and images are taken on the other side. Carrying measurements on both sides of the samples presupposes that there is no temperature gradient in the thickness of the sample which is reasonable considering Joule heating is performed.

2.5 Sample preparation

Samples are made of Armco iron. In the as-received state, grain size is around $15\mu m$. Material is austenized and maintained in temperature for two hours then cooled in oven. This treatments allows attaining grain sizes in the millimetre range. As the size of the grains are then of the same order of magnitude as the sample thickness, it seems acceptable to measure temperature and deformation on opposite faces of the sample. Moreover, some samples are deformed plastically prior to thermal testing in a range of strain varying from 1 to 10%. The objective is to characterize the influence of plasticity on the transformational behaviour.

To perform image correlation, a speckle pattern has to be applied to the surface of the samples. Following the recommendations of Dong et al. [7], alumina painting is applied on the sample using an airbrush with a fine nozzle. Figure 2 presents the studied zone of the sample as captured during experimental testing. The image is taken after one-minute heating at 1000K and it can be seen that there is no image degradation.

3 Modelling of allotropic transformation

3.1 Formulation of the model

In accordance with variational principles [8], a power functional whose stationarity conditions are equivalent to the thermomechanical problem to be solved is expressed and evolutions of variables are com-

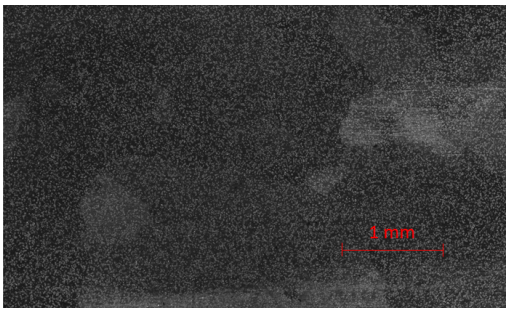

FIGURE 2 – Image of sample surface after 60 seconds heating at 1000K

puted through the optimization of this functional.
The model is written under the small strain assumption. The medium is modelled as a generalized standard material, which leads to a division of free energy into several terms that relate to elastically stored energy, plastically stored energy, thermal capacity energy and transformational energy respectively :

$$\Psi(\overline{\overline{\epsilon}}, \gamma_1, ..., \gamma_n, T, f) = \Psi_e(\overline{\overline{\epsilon}}, T, f) + \Psi_p(\gamma_1, ..., \gamma_n, T, f) + \Psi_{th}(T) + \Psi_{transfo}(f, T), \quad (2)$$

where the γ_i are the plastic slips on the different slip systems, be it for the BCC or FCC crystal configurations. f is the transformed volume fraction. It is introduced as an internal variable as in other works dealing with variational representation of phase changes in iron [9, 10]. Mechanical effect of phase transformation is a purely spherical contribution. This contribution is related to the dilatation associated with the change in lattice constants between the parent and product phases. Strain tensor reads :

$$\overline{\overline{\epsilon}} = \overline{\overline{\epsilon_e}} + f \times \overline{\overline{\epsilon_p}}_{BCC} + (1 - f) \times \overline{\overline{\epsilon_p}}_{FCC} + f \times \overline{\overline{\epsilon_T}} \quad (3)$$

where ϵ_T is transformation strain.

3.2 Single crystals behaviours

Slip systems are identified by the normal to the slip plane, $\overrightarrow{n_\alpha}$, and the slip direction inside this plane, $\overrightarrow{m_\alpha}$ (where α subscript refers to a given slip system). Resolved shear stress is expressed as :

$$\tau_\alpha = \overline{\overline{\sigma}} : \overline{\overline{P_\alpha}} \quad where\ \overline{\overline{P_\alpha}} = sym(\overrightarrow{n_\alpha} \otimes \overrightarrow{m_\alpha}). \quad (4)$$

In a rate-independent format, plastic slip occurs on the system when this variable reaches a critical value s_α. An expression is then needed for s_α to characterize hardening. An attempt is made to reproduce distinctly the behaviour of each phase. Besides, laws are chosen dependent on the densities of dislocations ρ_α to get more information on material behaviour at the mesoscale.
For the FCC phase, in which thermal effects play a minor role in opposition with the displacement of individual dislocations and their interactions with obstacles, a classical law for the evolution of critical shear stress is considered :

$$s_\alpha = s_{0_j} + \mu b \sqrt{\sum_\beta a_{\alpha\beta}\rho_\beta} \quad (5)$$

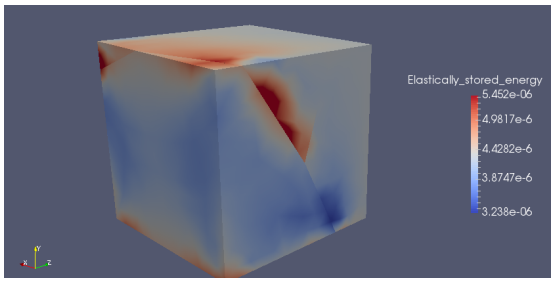

FIGURE 3 – Profile of the elastically stored energy (N.mm) in a cubic representative volume after 2% tensile deformation in the Y direction

s_0 is supposed to be constant and $\overline{\overline{a}}$ is the interaction matrix that accounts for the cooperation and competition between dislocations. To close the problem, an equation for dislocations evolution is introduced :

$$\dot{\rho_j} = \frac{1}{b}\left(\frac{1}{L_j} - 2y_c\rho_j\right)|\dot{\gamma_j}| \tag{6}$$

This relation expresses the competition between storage and annihilation processes. y_c is a characteristic distance of dislocations annihilation mechanisms and L is the mean free path of dislocations.
Behavior of the BCC phase exhibits a stronger temperature dependency. In the absence of obstacles, dislocations still need to overcome lattice friction. The limiting mechanism in BCC crystals is that they tend to form kinks along screw segments. To allow a displacement of the dislocation, thermal activation is then required. Besides obstacles also contribute to hardening and dislocations tend to acquire a jog when they intersect. Both ingredients are present in the model developed by Stainier et al. [11] which is used in this work.

3.3 Finite element simulations

Simulations are carried out using Zorglib finite element software, developed in-house at GeM. A volume heat source is introduced to model Joule heating. Radiation boundary conditions are applied on the free surfaces of the samples. Orientations of the different crystals are chosen randomly. Figure 3 presents an example of a simulation carried out on a 1-mm-side cubic sample which is representative of the microstructures observed experimentally. Displaying elastically stored energy highlights heterogeneities in the mechanical response of the material. More energy is stored near grain boundaries and triple junctions. Nucleation is then fostered in these particular locations. However, it can be noted that soliciting in tension the volume highly constrains external boundaries, hence performing calculations on it is less relevant than it would be on experimental geometries.

4 Conclusion

An experimental equipment suitable for high-temperature solicitations is designed. It allows the observation of iron samples during ferrite-to-austenite phase transformation without loss in image quality. Consequently, DIC computations can be performed in order to obtain strain fields. It paves the way for an in-depth characterization of microstructure evolution during transformation and for the determination of the influence of prior plastic activity on transformational behaviour. In parallel a numerical model is developed in the variational framework. It is constructed with a view on allowing a direct confrontation with correlation computations results. First test cases on representative volumes highlight mechanical discrepancies inside the material.

References

[1] Z.S. Basinski, W. Hume-Rothery and A.L. Sutton, The lattice expansion of Iron, Proceedings of the Royal Society A, 1955 .

[2] M.C. Casperson, J.D. Carroll, J. Lambros, H. Sehitoglu and R.H. Dodds Jr, Investigation of thermal effects on fatigue crack closure using multiscale digital image correlation experiments, International Journal of Fatigue, 2014 .

[3] P. Leplay, J. Réthoré, S. Meille and M. Baietto, Identification of asymmetric consitutive laws at high temperature based on Digital Image Correlation, Journal of the European Ceramic Society, 2012

[4] B. Swaminathan, W. Abuzaid, H. Sehitoglu and J. Lambros, Investigation using digital image correaltion of Portevin-Le Chatelier effect in Hastelloy X under thermo-mechanical loading, International Journal of Plasticity, 2015 .

[5] J.S. Lyons, J. Liu and M.A. Sutton, High-temperature deformation measurements using digital image correlation, Measurement Science and Technology, 1996 .

[6] B.M.B. Grant, H.J. Stone and M. Preuss, High-temperature strain field measurement using digital image correlation, Journal of Strain Analysis, 2009 .

[7] Y. Dong, H. Kakisawa and Y. Kagawa, Development of microscale pattern for digital image correlation up to 1400°C, Optics and Lasers in Engineering, 2015 .

[8] M. Ortiz and L. Stainier, The variational formulation of viscoplastic constitutive updates, Computational methods in Applied Mechanical Engineering, 1999 .

[9] A. Sadjadpour, D. Rittel, G. Ravichandran and K. Bhattacharya A model coupling plasticity and phase transformation with application to dynamic shear deformation of iron, Mechanics of Materials, 2015 .

[10] S. Yadegari, S.R. Turteltaub and A.S.J. Suiker, Coupled thermomechanical analysis of transformation induced plasticity in multi-phase steels, Mechanics of Materials, 2012 .

[11] L. Stainier, A.M. Cuitino and M. Ortiz, A micromechanical model of hardening, rate sensitivity and thermal softening in BCC single crystals, Journal of the Mechanics and Physics of Solids, 2002.